AGU PUBLICATIONS

Geophysical Research Letters

RESEARCH LETTER
10.1002/2014GL061478

Key Points:
- Radar interferometer observation of high-altitude meteor trail
- A new class of range-spread meteor trail echo at high altitude
- New perspective on the generation of high-altitude trail irregularities

Correspondence to:
G. Li,
gzlee@mail.iggcas.ac.cn

Citation:
Li, G., B. Ning, W. Wan, I. M. Reid, L. Hu, X. Yue, J. P. Younger, and B. K. Dolman (2014), Observational evidence of high-altitude meteor trail from radar interferometer, *Geophys. Res. Lett.*, *41*, 6583–6589, doi:10.1002/2014GL061478.

Received 8 AUG 2014
Accepted 11 SEP 2014
Accepted article online 13 SEP 2014
Published online 7 OCT 2014

Observational evidence of high-altitude meteor trail from radar interferometer

Guozhu Li[1,2], Baiqi Ning[1], Weixing Wan[1], I. M. Reid[3,4], Lianhuan Hu[1], Xinan Yue[5], J. P. Younger[3,4], and B. K. Dolman[3,4]

[1]Key Laboratory of Earth and Planetary Physics, Institute of Geology and Geophysics, Chinese Academy of Sciences, Beijing, China, [2]Beijing National Observatory of Space Environment, Institute of Geology and Geophysics, Chinese Academy of Sciences, Beijing, China, [3]ATRAD Pty Ltd, Adelaide, South Australia, Australia, [4]School of Chemistry and Physics, University of Adelaide, Adelaide, South Australia, Australia, [5]COSMIC Program Office, University Corporation for Atmospheric Research, Boulder, Colorado, USA

Abstract Whether radar meteor echoes occur at high altitudes (above ~130 km) in the Earth's atmosphere is a long-standing question within the meteor radar community. Using observations from the Sanya VHF coherent radar interferometer during 11 July to 10 August 2013, we have found a new class of range-spread high-altitude meteor trail echoes (HAMEs), some of which appeared at ~170 km altitude lasting more than 10 s. A statistical analysis on the local time dependence of the identified HAME events shows a maximum around 00–04 LT. The results imply that there could be much more meteor mass input due to meteoroid sputtering at high altitudes in the Earth's atmosphere than previously thought.

1. Introduction

Every day, innumerable meteoroids enter the Earth's atmosphere, colliding with surrounding air molecules to create columns of ionization, which constitute meteor trails. Observations from multiple instruments have shown that meteor trails generally occur below 130 km [*Ceplecha et al.*, 1998], with the exception of a few high-altitude optical meteors observed during the Leonid meteor shower [e.g., *Fujiwara et al.*, 1998; *Spurny et al.*, 2000].

More recently, observations from the European Incoherent Scatter (EISCAT) VHF radar reveal an unusual altitude distribution of meteor head echoes. A large number of head echoes were found to occur at high altitudes with a peak centered ~250 km [e.g., *Brosch et al.*, 2001, 2013, and the references therein]. This finding was investigated through a low-elevation north pointing experiment designed to investigate the effects of sidelobes on EISCAT meteor detection. *Vierinen et al.* [2014] argued that the high-altitude meteor echoes reported with the EISCAT radar are long range but normal-altitude (~80–130 km) meteor head echoes originating from the strong radar sidelobes and pointed out that "the mapping from radar range to actual target location can be made using interferometric receiver configuration through measuring the phase difference of the received echo by several nearby antennas." Since the reported high-altitude meteor echoes mostly come from EISCAT, which has failed to eliminate the range ambiguity of sidelobes [*Vierinen et al.*, 2014], more evidences from other radars, especially those with an interferometry capability, are urgently needed to unambiguously clarify whether and how often radar meteor echoes occur at high altitudes in the Earth's atmosphere. If the existence of high-altitude meteor trail echoes (HAMEs) is established, theoretical efforts can begin to explore the mechanisms responsible for high-altitude meteor ionization phenomena.

Unlike high-power, large-aperture (HPLA) radars, which are very sensitive to faint meteors within a very small beam width, lower power coherent radars usually have a significantly wider half-power (3 dB down) beam width but with less sensitivity and lower pulse repetition frequency (PRF). Meteor head echoes, which are frequently observed by HPLA radars [e.g., *Pellinen-Wannberg and Wannberg*, 1994], are difficult to be identified using wide-beam low-power radars. However, measurements from the Chung-Li and Sanya VHF coherent radars have proven that range-spread meteor trail echoes (RSTEs, also known as nonspecular echoes) produced by coherent scatterers from irregularities within meteor trails [*Chapin and Kudeki*, 1994; *Zhou et al.*, 2001; *Malhotra et al.*, 2007; *Oppenheim et al.*, 2008] can be observed by low-power coherent radars [e.g., *Chu and Wang*, 2003; *Li et al.*, 2012]. Specifically, an additional antenna array recently installed to the north of the main east-west array of the Sanya radar provides an interferometric capability to unambiguously determine the positions of irregularity echoes inside the 3 dB beam.

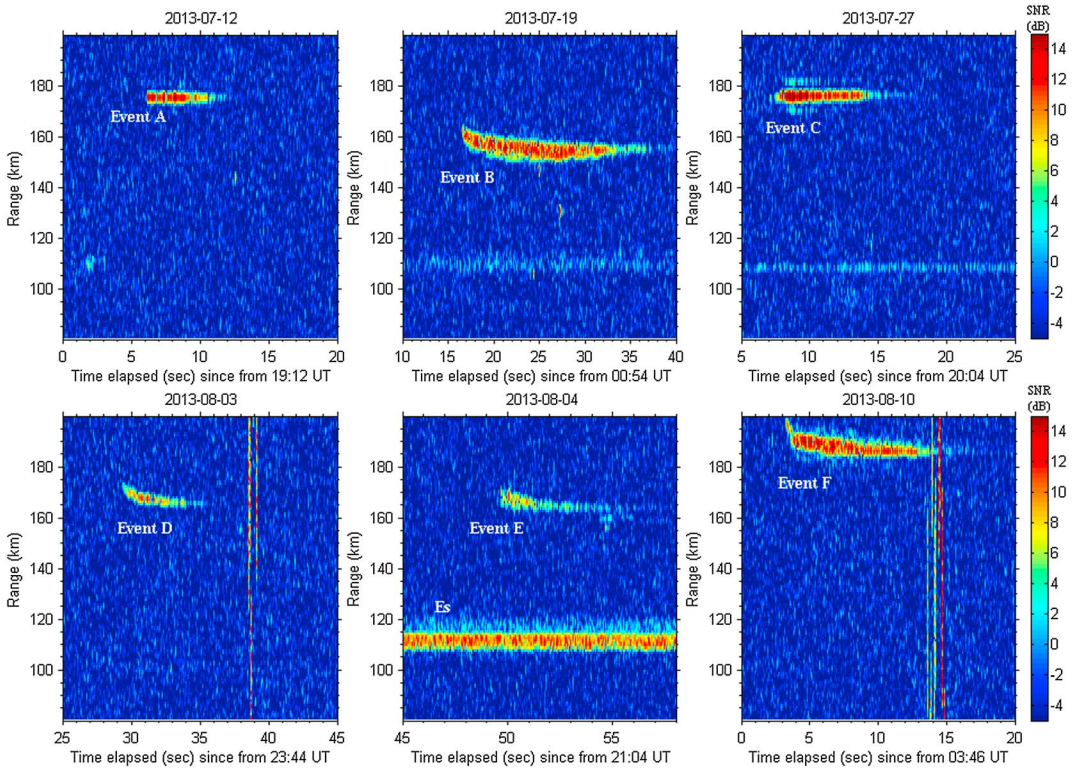

Figure 1. Typical examples (marked with A–F) of long-duration range-spread meteor trail echo (RSTE) lasting for 5–20 s. Note the strong E_s activity observed near 110 km range on 4 August 2013.

In this study, we present a class of range-spread high-altitude meteor trail echoes (HAMEs) detected with the Sanya VHF coherent radar interferometer during 11 July to 10 August 2013. These detections provide concrete evidence for the occurrence of radar meteor echoes at altitudes above 130 km. The HAME phenomenon raises questions about the formation and evolution of high-altitude meteor trail irregularities, as well as demonstrating the potential for studying high-altitude meteor trails with low-power interferometer equipped coherent radars.

2. Experiments

The 47.5 MHz Sanya VHF coherent radar (18.4°N, 109.6°E; dip angle 24.9° at 100 km altitude) has a phased antenna array comprised of six transmission/reception modules (each comprised of 2 × 2 Yagi antennas) spaced 8.93 m apart, aligned east-west. The radar transmits a peak power of 24 kW and is capable of detecting irregularities in the ionospheric *E*, valley and *F* regions, and meteor trails [e.g., *Li et al.*, 2012, 2013]. The most recent version of the Sanya radar produces a roughly elliptical 3 dB beam 16° × 36°, corresponding to a 42 km by 93 km half-power (3 dB) beam width at 150 km range.

Using the radar as part of an interferometer to determine the position of scatterers requires an additional receiving array that is spatially separated from the east-west array. For this purpose, one interferometric receive module was recently installed 17.86 m north of the east-west aligned main array to form a triangle with any two modules of the zonal baseline and hence provide the three-dimensional spatial interferometry capability.

In the experiment performed on 11 July to 10 August 2013, the main antenna beam of the Sanya radar was pointed north at a zenith angle of 24°. Observations were made at 2 min intervals, similar to that of *Li et al.* [2012]. As a result, a total of 30 data sets were recorded each hour. The radar PRF was 650 Hz, and the pulse length was 6 μs with a 4 bit complementary code. This corresponds to a range resolution of 0.9 km within the sampled range interval of 80–200.6 km. The received complex signals at every range gate were

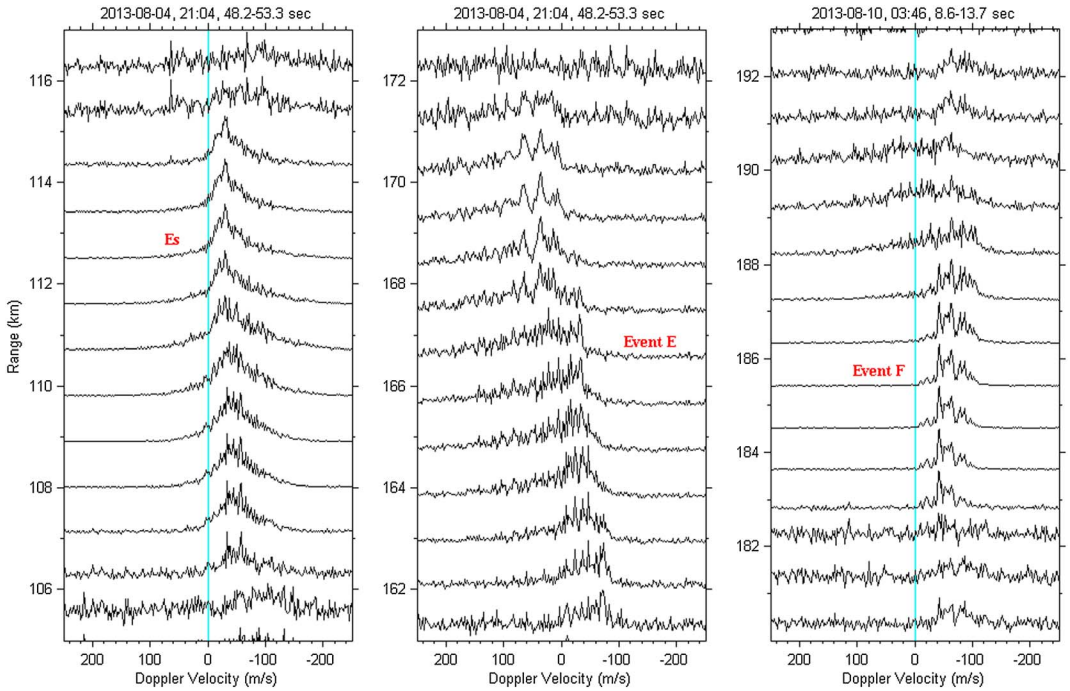

Figure 2. Examples of (left) Doppler spectra of sporadic *E* and of meteor trail events (middle) E and (right) F.

coherently integrated 4 times and used for offline interferometry analysis. All of the data, including the raw I/Q components used in this study, can be obtained from ftp://space.iggcas.ac.cn.

3. Results and Discussion

Figure 1 shows the range-time intensity maps depicting the signal-to-noise ratio of backscattered echoes recorded by the Sanya radar. Six meteor trail echo events (labeled A–F) above 150 km range are present. A sporadic *E* (E_s) irregularity layer centered near 110 km range is also clearly visible in the bottom middle panel of Figure 1, with weaker detections in the top middle and right panels.

It is clear from the figure that the meteor trail echoes, covering several range bins in similar manner to conventional RSTEs at lower altitudes, lasted for ~5–20 s. Before determining the real altitude that the trail echoes located through interferometry analysis, we classify these events as long-duration RSTE. The echo duration threshold for classifying long versus short trails varies from 5 s to over 1 min [e.g., *Malhotra et al.*, 2007; *Sugar et al.*, 2010; *Chau et al.*, 2014]. Here we choose a minimum duration of 5 s to classify long-duration trails [e.g., *Sugar et al.*, 2010].

Figure 2 shows the range variations of the self-normalized Doppler spectra of the E_s irregularity and the long-duration RSTE events E and F. Negative Doppler velocity indicates radial motion of the irregularity toward the radar. As can be seen from the figure, the Doppler spectral pattern of the E_s irregularity is different from those of the meteor trail events E and F. The meteor trail spectral pattern includes a broad asymmetrical wing to one side representing motions away from or toward the radar. The asymmetric wings of the spectra are very similar to those seen in Jicamarca radar observations [*Chapin and Kudeki*, 1994].

To determine the unambiguous position of the long-duration RSTEs shown in Figure 1, the phase differences of received echoes from all antenna array modules of the Sanya radar were employed in the interferometry analysis [*Farley et al.*, 1981]. The interferometer was comprised of two modules from the main east-west array and the additional module to the north. Different groups of noncollinearly aligned modules were used to improve the accuracy.

Figure 3 shows the positions of the RSTE events A–F and the E_s irregularity relative to the radar main beam direction at selected time intervals. In each plot the central black dot, the black ellipse, and the dash-dotted

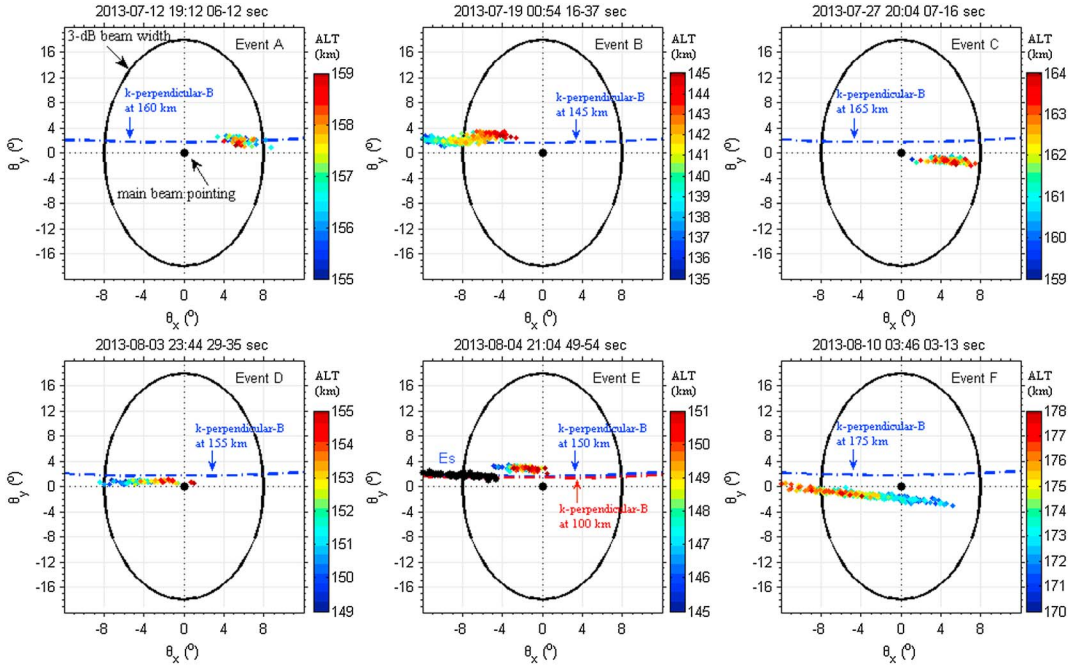

Figure 3. The direction of RSTE events A–F within the Sanya radar main beam, color-coded for altitude. The dash-dotted curve shows the direction perpendicular to the geomagnetic field (***k***-perpendicular-***B***) at a specific altitude, and black ellipse indicates the radar half-power (3 dB down) beam width.

line represent the radar main beam pointing, the radar half-power (3 dB down) beam width, and the direction perpendicular to the geomagnetic field *B* (***k***-perpendicular-***B***, ***k*** is radar wave number) at a specific altitude, respectively. Two notable features are clearly visible. The first is that the E_s echoes (shown in the bottom middle panel) appear along the curve perpendicular to *B*. This feature confirms the locus of the ***k***-perpendicular-***B*** region of the Sanya radar at ~100 km altitude in keeping with earlier results that the aspect sensitivity of E_s irregularities lies within 0.3° (off-perpendicular-*B*) [e.g., *Lu et al.*, 2008]. Second, the long-duration RSTE events C and F occur well away (~4°) from the ***k***-perpendicular-***B*** region of the Sanya radar, as well as being at extremely high altitudes (~160 km and 170 km, respectively). For the trail events A, B, D, and E, which occur below 160 km, the scatterers are located within 2° off-perpendicular-*B*. It is clear from the interferometric analysis that the long-duration RSTEs shown in Figure 1 are HAME events, which were produced by high-altitude meteor trail irregularities.

As part of the evaluation of RSTE events above 140 km range recorded during 11 July to 10 August 2013 by the Sanya radar, we performed a statistical analysis on the occurrence of HAME events. Figure 4a shows the distribution of HAMEs identified through manual inspection of the interferometry results as shown in Figure 3, plotted as a function of altitude and local time. The color-coded marks in Figure 4a represent the diurnal occurrence of HAMEs during the observational period (with a total number of 94). Since the frequent occurrence of strong summer E_s layer around 90–110 km altitudes over Sanya could cause an apparent reduction in the detection rate of trail echoes below 130 km altitude, a comparison of occurrence rates of conventional altitude RSTEs and HAMEs will be the subject of future work by using more interferometer observations on non-E_s days. Figures 4b and 4c show the local time (1 h interval) and altitude (5 km interval) histograms of the number of HAME events, respectively. It can be clearly seen that the majority of the events were observed below 160 km altitude with a maximum occurrence around 00–04 LT. The local time dependence of HAMEs is consistent with that of conventional altitude RSTEs detected by the Jicamarca radar, which are far more common at night than during the day [*Oppenheim et al.*, 2008]. From Figure 4c we note that there are 18 HAME events above 160 km. Since the upper range gate limit in the present experiment is 200.6 km (slant range), we cannot confirm whether the HAMEs can occur at altitudes higher than ~180 km or not. Additionally, it

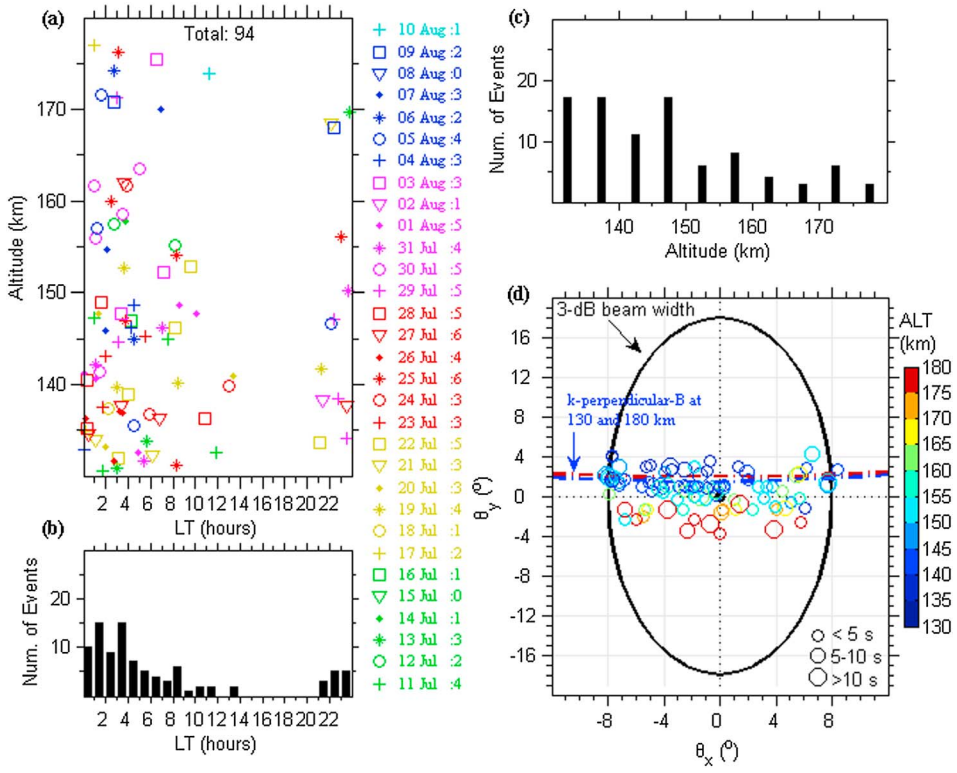

Figure 4. (a) The scatterplot of identified high-altitude meteor echo (HAME) events (a total of 94 above 130 km) in altitude versus local time. Notice the number of HAME events on a given day also present. (b, c) Histograms of all HAME events. It can be clearly seen that the HAMEs occur with a statistical preference during 00–04 LT. (d) Centroid trail positions of all HAME events, color-coded for altitude. The blue and purple dash-dotted curves show the directions of ***k***-perpendicular-***B*** at 130 and 180 km altitudes, respectively.

can be noted from the listed numbers of HAME events on given days that HAMEs were present on most days. This result implies a possibility that there is a population of meteor trails at higher altitudes in the Earth's atmosphere than previously thought possible according with the optical observations of meteor showers [e.g., *Spurny et al.*, 2000].

Comparing the centroid positions of HAME events that occur below 160 km altitude to that of HAME events above 160 km, a distinct pattern is apparent as shown in Figure 4d. In the plot, the size of the circles indicate the duration of the HAMEs, with small, medium, and large circles representing < 5 s (68 events), 5–10 s (16 events), and > 10 s (10 events), respectively. The finding of *Malhotra et al.* [2007] that long-duration RSTEs (for those appearing at 90–110 km altitudes) tend to occur near the ***k***-perpendicular-***B*** region is not seen. Note that *Malhotra et al.* used the duration threshold 15 s to classify long trails and found some of the RSTEs less than 10 s are located far from the ***k***-perpendicular-***B*** region. By steering the ALTAIR beam away from the ***k***-perpendicular-***B***, *Close et al.* [2008] examined the cutoff angle beyond which RSTEs are not detected. The authors found that the cutoff angle lies around 12° off-perpendicular-*B*, and the radar sensitivity to range-spread trails falls off 3 ± 2 dB per degree. From Figure 4d we note that there is a statistically significant preference for lower altitude HAME events (below 160 km) occurring near the ***k***-perpendicular-***B*** region of the radar.

Upon detection and confirmation of HAME events, the immediate questions are how meteor trails form at such high altitudes and how are the subsequent 3 m scale irregularities (plasma waves) responsible for the HAME generated within high-altitude meteor trails. Most meteoroid ablation is a thermal process whereby meteoroid kinetic energy is converted to heat via collisions with atmospheric molecules. At high enough temperatures, meteoroids evaporate, with some of the vaporized material being ionized by subsequent collisions [e.g., *Herlofson*, 1947]. This produces a column of plasma behind the meteoroid that constitutes the meteor trail.

However, at altitudes above ~130 km, the atmospheric density is too low for collisions to raise the temperature of the meteoroid enough for evaporation to occur. As a result, the classical ablation-ionization process responsible for the formation of normal meteor trails in the 70–110 km region cannot be responsible for the formation of meteor trails at the altitudes where HAMEs are detected. An alternative mechanism for the liberation of meteoric material is sputtering, which occurs when the relative kinetic energy of impacting atmospheric molecules exceeds the lattice energy of the meteoric material [*Brosch et al.*, 2001]. Under this condition, meteoric atoms may be ejected from the material lattice without evaporation. The sputtering process can result in nonnegligible meteoroid mass loss and the production of ionization at much higher altitudes than those associated with thermal ablation only [*Rogers et al.*, 2005]. Furthermore, a recent numerical simulation study on the electron production by *Mendis and Maravilla* [2009] highlighted the importance of physical sputtering as a dominant process for large and fast meteoroid at high altitudes. Our own numerical simulations of meteoroid ablation for a speed of 60 km s^{-1} with diameters of 1 mm and 1 cm indicate that sputtering can produce significant amounts of plasma up to 10^{12} electrons m^{-1} and 10^{14} electrons m^{-1}, respectively (J. Younger, private communication, 2014). Due to the low PRF of the Sanya VHF radar, no head echoes suitable for calculating the meteoroid velocity were identified in the data set. An analysis on the velocity of meteoroids responsible for HAME events will be addressed in the future.

For sufficiently dense meteor trails, the steep pressure gradients on the edges of a trail can supply energy to produce plasma waves and turbulence through Farley Buneman/gradient drift (FBGD) instability mechanism [e.g., *Dyrud et al.*, 2002; *Oppenheim et al.*, 2008, and references therein]. Turbulence drives the trail to form magnetic field-aligned irregularities that will be detected by radars as RSTEs.

The question of how 3 m scale irregularities could be generated within high-altitude meteor trail, producing echo durations in excess of 5 s, is difficult to answer at present. Since the favorable conditions for FBGD in meteor trails is limited to an altitude range of ~90–115 km [e.g., *Dyrud et al.*, 2002], FBGD instability is not sufficient to explain the occurrence of high-altitude RSTE. As mentioned above, the collisions between sputtered atoms moving at meteoric speeds and background atmospheric molecules have been suggested to lead to the generation of high-altitude meteor trails. By considering a minimum ionization rate of 1% in the sputtered materials from a large and fast meteoroid, *Rosenberg* [2008] proposed a possibility of lower hybrid (LH) instability driven by fast ions from a meteoroid traveling with a substantial component of velocity across $\boldsymbol{B}$. They concluded that LH waves, with wavelengths in the order of 10 m, could lead to some transient structures in the ionosphere. Some of the HAMEs detected by the Sanya radar with echo durations of less than 5 s might be the result of LH instabilities producing 3 m scale irregularities. However, for the HAMEs with longer durations of up to 10 s or more, the mechanism for producing the trails remains unclear. Numerical simulations of the formation of meteor trails, including mechanisms of high-altitude trail irregularities, are required. This should provide us with valuable insights into the formation and evolution of high-altitude meteor trails, as well as the occurrence of HAMEs.

4. Conclusions

The study has presented a class of range-spread meteor trail echoes appearing at high altitudes of up to ~170 km. The unambiguous altitudes of the trail echoes were determined by measuring phase differences of echoes between noncollinearly aligned antenna modules of the Sanya VHF coherent radar. These detections provide the first clear evidence of high-altitude meteor echoes in excess of 130 km. The local time dependence of the identified HAME events shows a similar behavior with that of RSTE detections in the normal meteor detection region. A statistically significant preference was found for HAME events below 160 km to cluster around the region perpendicular to the geomagnetic field, whereas most of the HAME events occurring above 160 km are located far away from the perpendicular-*B* region of the radar. A possible explanation on the occurrence of HAMEs is that sputtered materials from fast and/or large meteoroids produce high-altitude ionization trails, in which subsequent irregularities are generated through the lower hybrid instability mechanism. Long-duration HAME events lasting more than 5 s, however, need to be investigated further using numerical simulations to reveal potential instability processes.

Acknowledgments
This research is supported by the Natural Science Foundation of China (41422404, 41174136, 41374163, 41374164, and 41321003), Chinese Academy of Sciences (KZCX2-YW-Y10, KZZD-EW-01-3), and the National Important Basic Research Project of China (2011CB811405). The FTP access for the data used in this study can be obtained from L. Hu (hulh@mail.iggcas.ac.cn).

W.K. Peterson thanks Akshay Malhotra, Noah Brosch, and one anonymous reviewer for their assistance in evaluating this paper.

References

Brosch, N., L. S. Schijvarg, M. Podolak, and M. R. Rosenkrantz (2001), Meteor observations from Israel, in *Proceedings of the Meteoroids 2001 Conference, Kiruna, Sweden, 6–10 August 2001*, *Eur. Space Agency Spec. Publ., ESA SP-495*, edited by B. Warmbein, pp. 165–173, ESA Publications Division, Noordwijk, Netherlands.

Brosch, N., I. Haggstrom, and A. Pellinen-Wannberg (2013), EISCAT observations of meteors from the sporadic complex, *Mon. Not. R. Astron. Soc.*, *434*, 2907–2921, doi:10.1093/mnras/stt1199.

Ceplecha, Z., J. Borovicka, W. G. Elford, D. O. Revelle, R. L. Hawkes, V. Porubcan, and M. Simek (1998), Meteor phenomena and bodies, *Space Sci. Rev.*, *84*, 327–471, doi:10.1023/A:1005069928850.

Chapin, E., and E. Kudeki (1994), Radar interferometric imaging studies of long-duration meteor echoes observed at Jicamarca, *J. Geophys. Res.*, *99*(A5), 8937–8949, doi:10.1029/93JA03198.

Chau, J. L., I. Strelnikova, C. Schult, M. M. Oppenheim, M. C. Kelley, G. Stober, and W. Singer (2014), Nonspecular meteor trails from non-field-aligned irregularities: Can they be explained by presence of charged meteor dust?, *Geophys. Res. Lett.*, *41*, 3336–3343, doi:10.1002/2014GL059922.

Chu, Y.-H., and C.-Y. Wang (2003), Interferometry observations of VHF backscatter from plasma irregularities induced by meteor in sporadic E region, *Geophys. Res. Lett.*, *30*(24), 2239, doi:10.1029/2003GL017703.

Close, S., T. Hamlin, M. Oppenheim, L. Cox, and P. Colestock (2008), Dependence of radar signal strength on frequency and aspect angle of nonspecular meteor trails, *J. Geophys. Res.*, *113*, A06203, doi:10.1029/2007JA012647.

Dyrud, L. P., M. M. Oppenheim, S. Close, and S. Hunt (2002), Interpretation of non-specular radar meteor trails, *Geophys. Res. Lett.*, *29*(21), 2012, doi:10.1029/2002GL015953.

Farley, D. T., H. M. Ierkic, and B. G. Fejer (1981), Radar interferometry: A new technique for studying plasma turbulence in the ionosphere, *J. Geophys. Res.*, *86*(A3), 1467–1472, doi:10.1029/JA086iA03p01467.

Fujiwara, Y., M. Ueda, Y. Shiba, M. Sugimoto, M. Kinoshita, and C. Shimoda (1998), Meteor luminosity at 160 km altitude from TV observations for bright Leonid meteors, *Geophys. Res. Lett.*, *25*(3), 285–288, doi:10.1029/97GL03766.

Herlofson, N. (1947), The theory of meteor ionization, *Nature*, *159*, 444–454.

Li, G., B. Ning, L. Hu, Y.-H. Chu, I. M. Reid, and B. K. Dolman (2012), A comparison of lower thermospheric winds derived from range spread and specular meteor trail echoes, *J. Geophys. Res.*, *117*, A03310, doi:10.1029/2011JA016847.

Li, G., B. Ning, A. K. Patra, M. A. Abdu, J. S. Chen, L. Liu, and L. Hu (2013), On the linkage of daytime 150-km echoes and abnormal intermediate layer traces over Sanya, *J. Geophys. Res. Space Physics*, *118*, 7262–7267, doi:10.1002/2013JA019462.

Lu, F., D. T. Farley, and W. E. Swartz (2008), Spread in aspect angles of equatorial E region irregularities, *J. Geophys. Res.*, *113*, A11309, doi:10.1029/2008JA013018.

Malhotra, A., J. D. Mathews, and J. Urbina (2007), A radio science perspective on long-duration meteor trails, *J. Geophys. Res.*, *112*, A12303, doi:10.1029/2007JA012576.

Mendis, D. A., and D. Maravilla (2009), A note on the altitude profiles of the electron production in the atmosphere by micrometeoroids entering it at different initial speeds, *Geophys. Res. Lett.*, *36*, L22804, doi:10.1029/2009GL040908.

Oppenheim, M. M., G. Sugar, E. Bass, Y. S. Dimant, and J. Chau (2008), Day to night variation in meteor trail measurements: Evidence for a new theory of plasma trail evolution, *Geophys. Res. Lett.*, *35*, L03102, doi:10.1029/2007GL032347.

Pellinen-Wannberg, A., and G. Wannberg (1994), Meteor observations with the European incoherent scatter radar, *J. Geophys. Res.*, *99*(A6), 11,379–11,390, doi:10.1029/94JA00274.

Rogers, L. A., K. A. Hill, and R. L. Hawkes (2005), Mass loss due to sputtering and thermal processes in meteoroid ablation, *Planet. Space Sci.*, *53*, 1341–1354.

Rosenberg, M. (2008), On the possibility of a lower-hybrid instability driven by fast ions sputtered from a meteoroid, *Planet. Space Sci.*, *56*, 1190–1193.

Spurny, P., H. Betlem, J. Vant Leven, and P. Jenniskens (2000), Atmospheric behavior and extreme beginning heights of the thirteen brightest photographic Leonid meteors from the ground based expedition to China, *Meteorit. Planet. Sci.*, *35*, 243–249.

Sugar, G., M. M. Oppenheim, E. Bass, and J. L. Chau (2010), Nonspecular meteor trail altitude distributions and durations observed by a 50 MHz high-power radar, *J. Geophys. Res.*, *115*, A12334, doi:10.1029/2010JA015705.

Vierinen, J., J. Fentzke, and E. Miller (2014), An explanation for observations of apparently high-altitude meteors, *Mon. Not. R. Astron. Soc.*, *438*, 2406–2412, doi:10.1093/mnras/stt2358.

Zhou, Q.-H., J. D. Mathews, and T. Nakamura (2001), Implications of meteor observations by the MU radar, *Geophys. Res. Lett.*, *28*(7), 1399–1402, doi:10.1029/2000GL012504.